Review Article

Yang Wang, Dan Lei, Liangke Wu*, Rongkun Ma, Huiming Ning*, Ning Hu, and Alamusi Lee

Effects of stretching on phase transformation of PVDF and its copolymers: A review

https://doi.org/10.1515/phys-2022-0255
received February 14, 2023; accepted May 26, 2023

Abstract: Poly(vinylidene fluoride) (PVDF) and its copolymers are promising candidates for energy-harvesting devices because of their flexibility, environmental friendliness, lightweight, and high halogen and acid resistance. However, the relatively low piezoelectricity limits their applications. The piezoelectricity of PVDF and its copolymers highly depends on the polar β-phase, while the non-polar α-phase is the most common one. As a result, the β-phase formation and α- to β-phase transformation have attracted much attention in recent years. Stretching is a widely used method to induce the α- to β-phase transformation for the improvement of piezoelectricity. In this work, the influences of the parameters during stretching on phase evolution and piezoelectricity are discussed and summarized. Besides, nontraditional stretching methods are also introduced and discussed. This work will provide important information for preparing high-performance piezoelectric polymer films.

Keywords: PVDF, mechanical stretching, nontraditional stretching

Nomenclature

PVDF	poly(vinylidene fluoride)
XRD	X-ray diffraction
v	drawing speed
T_s	stretching temperature
R	elongation ratio
$F(\beta)$	relative fraction of the β-phase
X_c	crystallinity degree
TCD	tip-to-collector distance

*** Corresponding author: Liangke Wu**, College of Aerospace Engineering, Chongqing University, Chongqing 400044, China, e-mail: wuliangke@cqu.edu.cn, tel: +86-02365102510
*** Corresponding author: Huiming Ning**, College of Aerospace Engineering, Chongqing University, Chongqing 400044, China, e-mail: ninghuiming@cqu.edu.cn
Yang Wang, **Ning Hu:** College of Aerospace Engineering, Chongqing University, Chongqing 400044, China
Dan Lei: AECC Guizhou Honglin Aero-engine Control Technology Co., Ltd, Guiyang 550025, China
Rongkun Ma: Shanghai Road and Bridge (Group) Co., Ltd., Shanghai 200433, China
Alamusi Lee: School of Mechanical Engineering, Hebei University of Technology, Tianjin 300401, China

1 Introduction

As potential energy-harvesting materials, poly(vinylidene fluoride) (PVDF) and its copolymers have great advantages such as excellent processing ability, corrosion resistance to acids and alkali, flexibility and thermal stability. PVDF possesses at least five polymorphs, among which the β-phase is the most important one due to its high piezoelectricity. In the initially prepared PVDF films, the non-polar α-phase usually dominates, which does not contribute to piezoelectricity. In order to obtain high-piezoelectric PVDF films containing a high content of the β-phase, a number of methods including stretching, nanofiller addition, poling, and heat treatment have been developed [1–5].

The addition of fillers is widely used to improve the piezoelectricity of PVDFs. In 2020, Chamakh *et al.* added ZnO star-like fillers ($d \approx 2.5$ μm) into PVDF and investigated its effects on the structural and physical properties. The β-phase fraction increases from 44.1 to 66.4% after the addition of 10 wt% ZnO microparticles [6]. Compared to microfillers, nanofillers have unique advantages due to their large specific area. In recent years, various nanofillers (carbon nanotubes, vapor-grown carbon fibers, graphene, graphene oxide [GO], metal nanowires, ionic liquid, *etc.*) have been utilized as reinforcing agents. The enhancement mechanism includes nucleate agents and the interaction between the molecular chains and the nanofillers [4,7,8]. The effects of poling include α- to β-phase transformation and the realignment of dipole moments. In the prepared films without poling, the dipole moments are randomly distributed; thus, the total piezoelectricity is extremely weak or does not exist because of the mutual offset of the dipole moments. During the poling process, the applied

high electric field can force the dipole moments to align along the electric field direction, thus inducing piezoelectricity [9–11]. Heat treatment can affect the crystallization process, and thus, proper heat treatments can also result in high β-phase [12,13].

Compared with the above-mentioned methods, stretching has obvious advantages in the α- to β-phase transformation. Phase transformation needs external energy to overcome the energy barrier between the phases. In the poling process, although there is stress applied to the molecular chains, it is an order lower than that of stretching, and thus not enough external energy can be provided. Limited by the breakdown strength, the poling electric field cannot be higher than the ultimate value (usually lower than 150 MV/m); therefore, stretching is a more efficient method to promote crystal phase transformation [14,15]. It should be noted that the piezoelectricity not only depends on the fraction of the electric active β-phase, but also the alignment of the dipole moments is also very important. Therefore, the crystallographic plane orientations should be carried out by high electric poling or other methods, which is not discussed in detail due to the length limit. In some reports, the enhancement of β-phase is considered equal to the enhancement of piezoelectricity, while the following processes are not mentioned.

Traditional mechanical stretching has the advantages of low cost, simple, and practicable. Different from traditional mechanical stretching, the simultaneous poling and stretching process has also been developed. In addition, the stretching process also exists in electrospinning, which has characteristics of simplicity, low cost, and beneficial to small diameters. But the promotion of electrical instabilities within a charged fluid jet and a long jet path in solvent evaporation readily result in nanofibers and ultra-fine fibers. To solve this problem, researchers have developed a technology similar to electrospinning, namely melt electrowriting (MEW), which is distinct from electrospinning as the electrical instability is suppressed due to precisely placed fibers, which can keep a fluid column against breaking at low flow rates. However, it might require high pressure to extrude the material when the filler content is high, which are not achievable by pneumatically driven MEW printers, or lead to nozzle clogging [16,17]. In this work, the influences of stretching parameters on the phase transformation of PVDF and its copolymers are discussed in detail and summarized. Our work will provide a solid foundation for the development of perfect piezoelectric polymers and composites.

2 Influences of the parameters of stretching on the α- to β-phase transformation

2.1 The α-to β-phase transformation mechanism during stretching

During the stretching process, the transformation process from α-crystal to β-crystal of PVDF by mechanical stretching is revealed and is summarized schematically in Figure 1. The α spherulite of PVDF with folded chains can be readily obtained under conventional processing conditions (Figure 1a). When mechanical drawing is applied on the polymer, the transition starts from the middle of the spherulite, where the molecular chains are first extended along the drawing direction (Figure 1b). With the deformation of the α-phase, the conformation is formed in the emerged β-phase gradually (Figure 1c). More and more extended chains formed with the evolution of the deformation of PVDF; therefore, the α-phase transforms into the β-phase under large deformation (Figure 1d). The above is the recrystallization process inside PVDF during stretching [18]. The recrystallization process is also affected by the temperature, as discussed in Section 2.2.1.

Compared to non-stretched films, the stretched films usually contain a much higher content of β-phase $F(\beta)$ [19]. The α- to β-phase transformation mechanism during stretching can be described as follows: (1) The applied stress along the stretching direction forces the spherical crystal into a microfiber-like crystal and (2) the fiber-like structure is beneficial for the formation of the TT conformation (β-phase) than the TGTG′ conformation (α-phase). However, the effect of stretching on the crystallinity degree varies with specific processes. Both

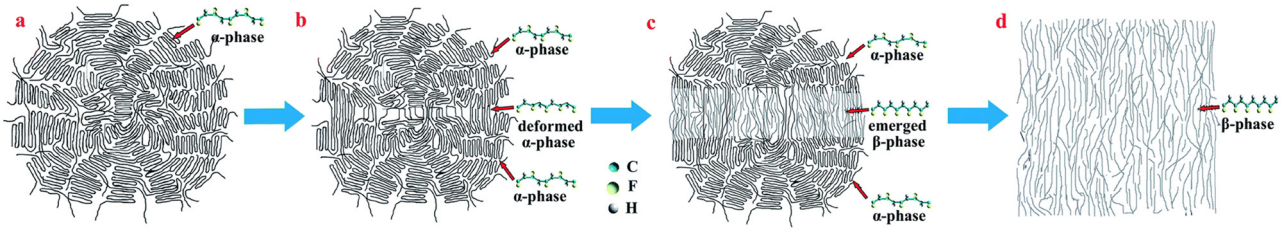

Figure 1: Schematic drawing of the transformation process from α-crystal to β-crystal of PVDF by mechanical stretching [18].

increment [20,21] and decrement [22,23] have been reported. The increment in the crystallinity degree after stretching may be attributed to the alignment of molecular chains along the stretching direction, and thus, the microcrystalline zone is formed, resulting in the formation of the crystal structure. In contrast, stretching may also destroy the current crystal structure and lead to the formation of a semi-crystal zone, which reduces the crystallinity [22–25]. In the stretched films, the molecular chains mainly align along the stretching direction. Therefore, it is good to work at the *31* mode after subsequential poling.

The parameters of mechanical stretching include the stretching temperature (T_s), elongation ratio (R), and stretching speed (v). Besides, the addition of nanofillers can also affect phase evolution, as discussed in Section 2.2.

2.2 Influences of stretching parameters on the phase transformation

2.2.1 Stretching temperature (T_s)

Temperature is an extremely important factor affecting phase transformation. In some reports, the samples are kept at a certain temperature for a short time before and/or after stretching for preheating or eliminating internal stress [26]. Mun *et al.* stretched the PVDF hollow fiber membranes by 1.5 times for 60 s. Before stretching, the films were kept in distilled water at 60°C for 60 s. After stretching, the annealing process at 50–120°C was applied. It was found that the relative fraction of the β-phase $F(\beta)$ reached 68.9% and the crystallinity degree was 44.4% when the stretching temperature was 60°C. However, the tensile strength was the lowest [27]. Temperature above 100°C may reduce phase transformation efficiency. When the temperature is above 120°C, the transformation will not occur even when the elongation ratio is higher than 4. The crystallinity degree may increase significantly, and the crystal–amorphous interphase region may be reduced because of the increase of the thickness of the crystalline layer induced by the stretching process [28–30]. Kim *et al.* stretched the PVDF hollow fiber membranes at a temperature from 30 to 90°C. It was found that 60°C is the right temperature, at which the relative fraction of the β-phase $F(\beta)$ may reach 70%. Lower or higher temperatures lead to lower $F(\beta)$ [31]. Sencadas *et al.* investigated the α- to β-phase transformation during the stretching process at different temperatures (80–140°C). They studied the stress–strain relationship for the samples stretched at 80°C, as shown in Figure 2(a). With the increase of R, the samples undergo three stages subsequently: yielding, necking, and

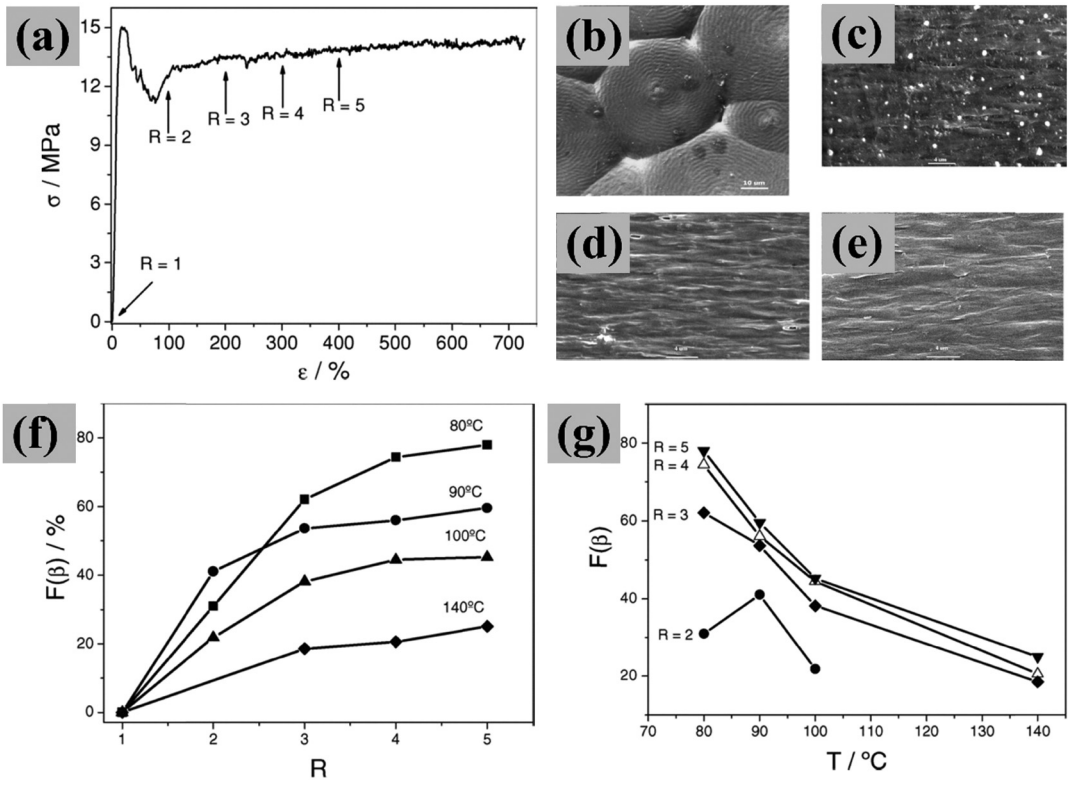

Figure 2: (a) Stress (σ)–strain (ε) curve for an original α-PVDF sample uniaxially stretched at 80°C. Scanning electron microscopy (SEM) micrographs obtained from samples stretched at 80°C: (b) R = 1, (c) R = 3, (d) R = 4, and (e) R = 5. $F(\beta)$ as a function of stretching ratio R (f) and stretching temperature T_s (g) [32].

strain hardening. The maximum stress existed at the post-yield softening and a plastic plateau before rupture ($R \approx 8$). With stretching, the crystal structure and the phase transformation proceed. For larger deformation, the microscopic deformation mechanism is characterized by the transition from the spherulitic structure to the microfibrillar structure accompanied by the destruction of the lamellar morphology. As mentioned above, PVDF with folded-chain α-spherical crystals can be easily obtained under conventional processing conditions. During stretching, necking and thickness reduction occur in the films. Foldable α-spherical crystal is extended along the stretching direction and gradually spreads toward the unstretched area, *i.e.*, the fragmentation of the crystalline area inside the PVDF matrix. As the deformation occurs, the area of the extended chains expands laterally from the middle of the spherulite. Accompanied with it, the α spherical structure transforms into a microfiber structure, and small blocks of lamellae are torn away from the original lamellae to form a fibrillar structure, which is corresponding to the β-phase. This mechanism induces all-trans planar zigzag conformation into the crystals. Overall, the stretching process is the destruction and reorganization of the internal crystalline region, as shown in Figure 2(b)–(e). For all the samples, $F(\beta)$ increases with R and reaches a plateau near 5. In contrast, $F(\beta)$ decreases with temperature, as shown in Figure 2(f)–(g). The temperature increment may decrease the viscosity, leading to the matrix being more ductile [32].

In order to investigate the mutual influences of T_s and R, Ting *et al.* investigated the influences of biaxial stretching on the piezoelectricity of PVDF thin films by varying the stretching ratio and temperature. From SEM images, the uniformity in the biaxial direction is confirmed. However, the high stretching ratio ($R = 4 \times 4$) can induce porosity and cracks, though it shows better surface chain orientation and smoothness. To avoid crystal defects, the elongation ratio is suggested to be set in between $R = 3 \times 3$ and $R = 4 \times 4$. The β-phase fraction $F(\beta)$, crystallinity degree and piezoelectric coefficients (d_{31} and d_{33}) of the samples decrease with the temperature for all samples ($R = 2 \times 2$, $R = 3 \times 3$, $R = 4 \times 4$, $R = 5 \times 5$) when the temperature is above 80°C [33]. Li *et al.* studied the transformation from α- to β-crystal of the PVDF membrane that is carried out under the conditions of different stretching temperatures, stretching rates, and tensile elongation. The stretched films were characterized by Fourier transform infrared (FTIR) spectroscopy and X-ray diffraction (XRD) to analyze quantitatively the transformation from α- to β-crystal. The results indicate that low temperature is conducive to the formation of the β-crystal and the stretching temperature around 100°C is suitable for the transformation under stretching. With the increase of the tensile elongation, the relative crystallinity would also increase and achieve a maximum value when R is above 3. However, the stretching rate has less effect on the transformation from α- to β-crystal [34]. Debili *et al.* analyzed the stretched films under different temperatures (75, 80, 90, 100, and 110°C) with $R = 4$ by FTIR and XRD techniques. It was observed that a relatively low temperature (80 and 75°C) induces higher β-phase, while at higher temperatures, the transformation is not sufficient. It is because the semi-nanocrystalline biphasic (α + β) system is formed in the samples stretched at $T_s >$ 80°C. In contrast, the single nanocrystalline β-phase is formed when $T_s \leq 75$°C [34]. The addition of nanofillers also affects the crystal structure in the prepared films. Lee investigated the influences of temperature on the crystal structure and thermal properties of PVDF-HFP/CNF (0.2 wt%) by uniaxially stretching the films ($R = 4.5$) at 50, 75 and 100°C, respectively. The SEM images confirm the orientation of the CNF and the PVDF-HFP matrix. In the SEM images, the aggregation of CNFs in the matrix is observed in the undrawn samples. When the samples are drawn at 50°C, the PVDF molecular chains align along the stretching direction partially, and it is improved in the samples drawn at 75°C. The samples drawn at 100°C show partial melting of the matrix and wrapping in the CNFs, as shown in Figure 3(a)–(d) [21].

Guo *et al.* investigated the stretching-induced phase evolution of PVDF/Gr composites by X-ray scattering. The results show that the α- to β-crystal transformation is based on the orientation evolution of molecular chains and it would not occur when R is less than the threshold value of 1.5. It is concluded that the α- to β-phase transformation goes through an indirect approach *via* the intermediate state of stretching-induced fragmentation and recrystallization process, rather than a direct evolution, as shown in Figure 4. When T_s is 30°C, the adequate concentrated stress on the crystal phase results in the β-phase formation from the initial recrystallization. While in stretched films at 160°C, the α- to β- phase transformation is hindered, which is attributed to the worse compatibility of PVDF and Gr and the high chain mobility at a higher temperature [35]. It is different from most reports in which stretching is carried out from 60 to 100°C, so the effect of temperature is highly dependent on the specific process.

2.2.2 Elongation ratio (*R*)

The elongation ratio is another decisive factor in the stretching process. Generally, $F(\beta)$ increases with the elongation ratio due to the formation of the fiber-like structure of β-phase molecular chains by the applied stress [36]. It may also cause problems such as structural defects and

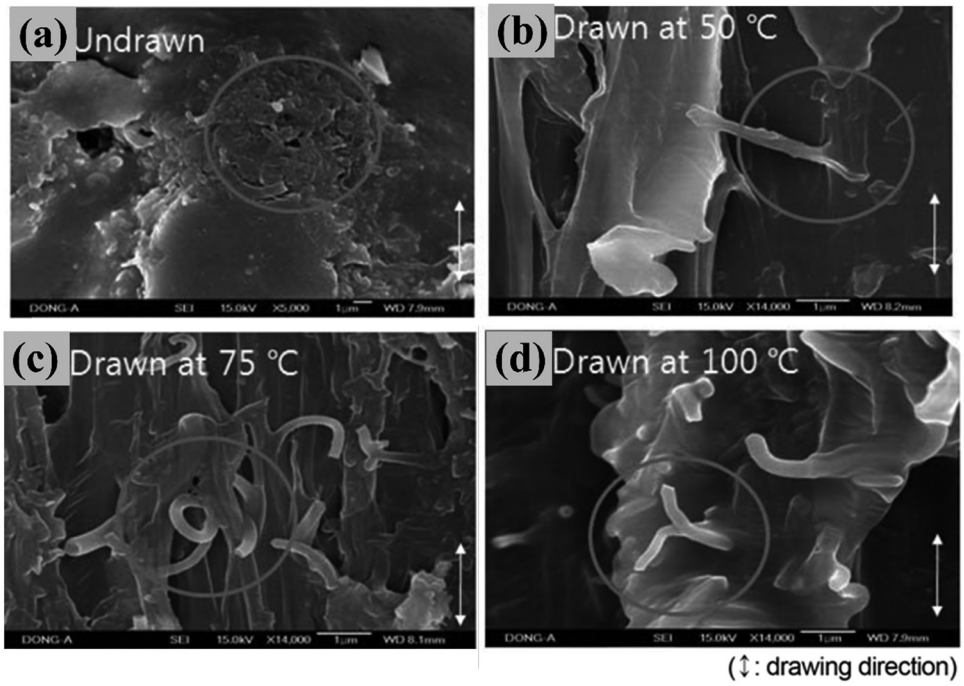

Figure 3: SEM images of CNF/PVDF-HFP composite films at various stretching temperatures: (a) undrawn, (b) drawn at 50°C, (c) drawn at 75°C, and (d) drawn at 100°C [21].

decrease of crystallinity [23,37]. During the stretching process, the molecular chains are forced to be elongated, and thus, the β-phase is preferred (a(α) = 0.496 nm; a(β) = 0.858 nm). Zhou *et al.* prepared PVDF/PMMA blend films by biaxial stretching and investigated the effects of the PMMA content and elongation ratio on the crystallinity degree and the β-phase fraction. The results show the presence of the β-phase in the initial crystallized PVDF/PMMA blend films, while F(β) decreases in the pre-heating process. During biaxial stretching, F(β) shows an increasing trend and reaches the maximum value of 93% in PVDF/PMMA (30 wt%) with an elongation ratio R = 2 × 2. It is remarkable that both the reduction of the PMMA content and the increase of the stretching ratio improve the crystallinity degree. The interaction between –C═O groups (PMMA) and $-CH_2$ groups (PVDF) can also induce β-phase formation. Compared to uniaxial stretching, the stress distribution is more uniform, leading to the uniform distribution of the β-phase fraction [38]. Chang *et al.* investigated the phase transformation of PVDF by a micro-testing machine. It was found that the phase transformation increases with the elongation ratio until 4 and then stays at a plateau. Therefore, for PVDF films, the elongation ratio R = 4 is enough for the α- to β-phase transformation [39]. Ji *et al.* prepared PVDF hollow fiber membranes by a green melt-spinning and stretching process without an organic solvent and low-molecular-weight diluent. The effect of elongation ratio was investigated by SEM, as shown in Figure 5. It is obvious that with the increase of the elongation ratio, the micro-structure of PVDF becomes fiber-like, which is preferred to form the β-phase [40]. Ozkazanc *et al.* investigated the effects of the elongation ratio on structures stretched at a constant speed (0.005 mm/s) at 155°C (a temperature much higher than that usually reported). It was found that with the increase of the elongation ratio, the specific volume in the amorphous phase decreases [41,42]. The crystallinity degree may increase with the elongation ratio [43,44]. Wang *et al.* fabricated high-piezoelectric PVDF films (reverse piezoelectric coefficient: −37 pC/N) by mechanical stretching of the initial crystallized films coated on stretchable poly(vinyl alcohol) substrates with a speed of 80 μm/s at 110°C. The AFM images show that the stretching process results in parallel strip-like structures along the stretching direction, indicating the formation of the extended β-phase. R = 3 is sufficient for phase transformation, while higher R (5) may cause problems such as higher roughness and crystal defects [44]. For biaxial stretching samples, the increase of F(β) has also been observed in biaxial stretching, and a maximum value of 84% is reached at R = 4 × 4 [33]. The phase transformation during the stretching process begins from the middle of α-spherulite and then extends to the neighboring spherule with the increase of the elongation ratio. F(β) increases with the elongation ratio until 3 and then stays at the plateau, indicating R = 3 is enough for sufficient α- to β-phase transformation [34]. Jain *et al.* investigated F(β) and X_c under

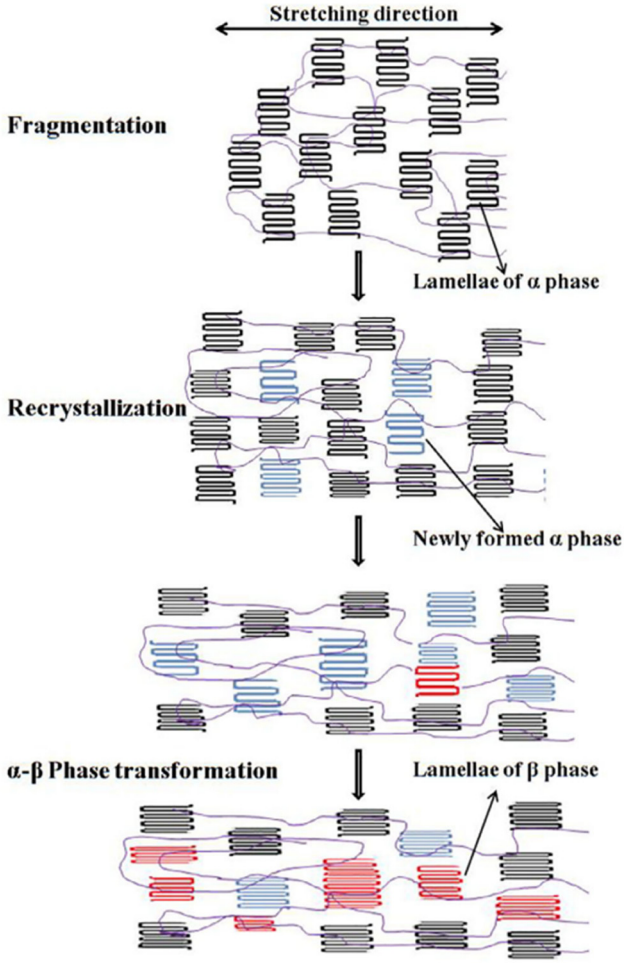

Figure 4: Schematic diagram of the PVDF/Gr structure evolution induced by tensile deformation [35].

different stretching conditions by XRD, differential scanning calorimetry (DSC), and FTIR techniques. It was found that both the crystallinity degree X_c and $F(\beta)$ increase with the stretching temperature until 80°C and then decrease [45].

In summary, for sufficient stretching, R should be at least 3, and in most cases, it exceeds 4. Combined with a moderate temperature, the effects of stretching can be improved. As is well-known, the crystal structure is highly related to the temperature. During stretching, the high temperature can increase the mobility of molecular chains, which makes the stretching more easy and prevents the fracture. However, the ultra-high temperature may result in a decrease in crystallinity degree and β-phase fraction [44,45].

2.2.3 Speed (v)

Speed is also a key factor affecting phase formation. In the current research, the conclusions about the drawn rate on the phase evolution in the reports vary greatly due to differences in experimental techniques and environments. Magniez *et al.* developed high-β-phase PVDF fibers by a melt-spinning method through unidirectional stretching at 120°C with different elongation ratios (1.25, 1.5, and 1.75). It was found that the β-phase fraction increases with the elongation ratio regardless of the flow rate. When the elongation ratio remains unchanged, the β-phase fraction decreases with the flow rate [46]. In contrast, for hard elastic films prepared by casting or hot pressing methods, when they are subjected to uniaxial stretching, a low stretching rate may lead to insufficient initial layer separation, while an excessively high stretching rate may lead to the destruction of the crystalline region inside the PVDF. However, there is currently significant controversy on the impact of the stretching rate on the internal phase transition and crystallinity of the film. Lei *et al.* investigated the crystalline morphology and microstructure during the stretching of PVDF hard elastic films under room temperature at different strain rates (0.003–0.034 s^{-1}). It was found that the β-phase content decreases with the strain rate when it increases from 0.003 s^{-1} (39.8%) to 0.017 s^{-1} (9.8%) but increases with the strain rate to 0.034 s^{-1} (26.3%). In other words, when the strain rate is below 0.003 s^{-1}, it is not sufficient to separate the initial lamellae. When the strain rate is >0.003 s^{-1}, the lamellae separation occurs, leading to the lower β-phase content. For a higher faster rate (such as 0.034 s^{-1}), the stress can induce sufficient fragmentation and reorganization of thinner crystals, leading to higher β-phase content [47]. In other reports, the higher the strain rate, the higher the phase transformation, which is completely different from other published reports [48,49]. Li *et al.* studied α- to β-phase transformation under different conditions (T_s, R, and v). In their experiments, the speed (0.06, 3, 6, 12, and 60 mm/min) has little impact on the transformation, which is completely different from other reports [18]. Regarding crystallinity, it was reported that speed can have a significant effect on it. Lee and Cho stretched PVDF/CNF films (T_s = 125°C, R = 4) at various speeds and measured their crystallinity. It was found that with the increase of the temperature, the crystallinity degree decreases gradually (100% min^{-1}: 50.5%; 5,000% min^{-1}: 40.2%) [50]. Tang *et al.* also reported similar results [51].

In summary, the impact of the stretching rate on the crystal phase transition and crystallinity of thin films is controversial in current reports. As PVDF is a thermoplastic material, the ductility and elastic modulus of the film are usually temperature dependent. At room temperature, the film has low ductility and low internal molecular activity, and the phase transition of the film will start only when the tensile rate reaches a certain threshold. When

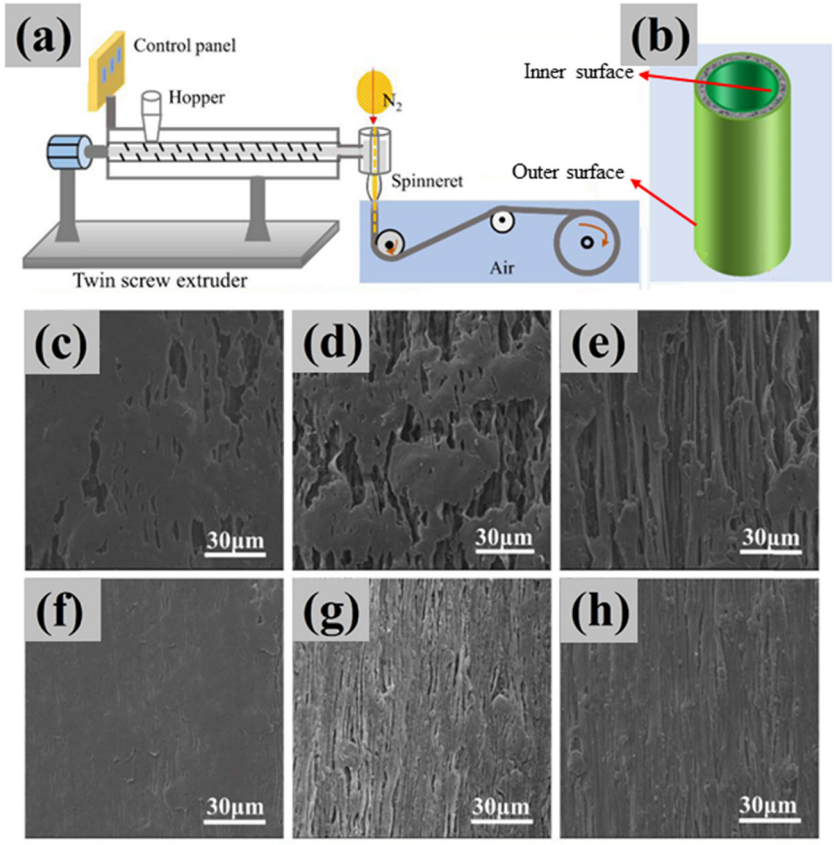

Figure 5: (a) Schematic description of the preparation process of the melt-spinning hollow fiber membranes. (b) The prepared nascent hollow fibers. The SEM images of the prepared hollow fiber membranes with different elongation ratios: (c) R = 1, outer surface; (d) R = 2, outer surface; (e) R = 3, outer surface; (f) R = 1, inner surface; (g) R = 2, inner surface; and (h) R = 3, inner surface [40].

the stretching temperature is higher, the mobility of molecular chains in PVDF is higher and the stretching rate has little effect on the phase transformation; however, if the stretching rate is very high, the crystallinity degree will decrease significantly.

2.2.4 Nanofiller addition

The addition of nanofillers is a widely used method to prepare PVDF-based composites with a high β-phase fraction [52–55]. The nanofillers mainly work in the initial crystallization stage as nucleate agents, which is beneficial for the direct formation of the β-phase. As a result, the relative β-phase fraction $F(\beta)$ is quite high in the prepared films containing a high content of nanofillers [20]. Thus, the α- to β-phase transformation is not so obvious in the subsequent stretching process. While for those samples containing lower nanofillers (<threshold value), there is an improvement, which is attributed to the stress concentration (the stretching force tends to be centralized in the nanofiller/PVDF interface). In contrast, when a neat PVDF film is stretched, the stretching force only works on the molecular chains [22]. Mishra *et al.* investigated the effects of mechanical stretching on the β-phase formation in PVDF/rGO and PVDF/GO composites. The maximum $F(\beta)$ reaches about 85% (PVDF/GO(0.5 wt%), R = 2, $F(\beta)$ = 86%; PVDF/rGO(1 wt%), R = 2, $F(\beta)$ = 84), accompanied with dramatically improved dielectric properties. Compared to non-stretched films, it is more than a 10% increase. This behavior is attributed to the strong interaction between PVDF and GO or rGO, *i.e.*, the maximum stress is applied during the stretching process. The dielectric constant (highly related to the piezoelectricity) also increases with the addition of nanofillers [23]. He *et al.* prepared PVDF/organosilicate (OS) composites containing 2 and 4 wt% OS and investigated the effects of added nanofillers. Based on previously published reports, it was concluded that the improvement effect of OS is induced by the electrical interfacial interactions between the positively charged OS surface and the partially negative $-CF_2$ bonds of the PVDF molecular chains, as shown in Figure 6 [20]. Yu and Li stretched PVDF/Ni composites at

120°C and investigated the effects of the stretching ratio on the dielectric properties. The results indicated that the addition of Ni particles can strengthen the interaction between Ni particles and the polymer matrix, and thus, the samples containing more Ni nanofillers exhibit a higher rupture ratio and stretching-induced percolation threshold [56]. The stretching process realigns the molecular chains and the added nanofillers attribute to the space-charge accumulation at the two-phase boundary during the stretching process [56]. Jahan *et al.* explored the polar phase transformation and the crystallinity degree of PVDF/$CaCO_3$/clay composites affected by the $CaCO_3$ fraction and elongation ratio. It was confirmed that the addition of fillers could improve the formation of the β-phase. For stretched (T: 90°C, R: 4–5) samples containing high filler contents (>2 wt% clay), the β-phase predominates regardless of R, and the α-phase even disappears. It means that the added fillers play a significant role in the β-phase formation during the stretching process because of its nucleate effect, which can hinder polymer mobility during melt crystallization, and therefore, more extended chain β-crystals are more easily formed. The added fillers may lead to the decrease of the crystallinity degree, which plays a negative role in piezoelectricity improvement [43].

Molecular weight (M_w) is important for PVDF's properties. Mrlík *et al.* systematically studied the effects of main parameters such as molecular weight, initial sample thickness, stretching and poling. It was found that the highest degree of β-phase (90%) was realized with a moderate molecular weight (M_w = 275 kDa) and the highest axial elongation (500%). In the low elongation ratio (<500%) stretching, the piezoelectric charge coefficient d_{33} is highly dependent on the M_w, while with higher elongation ratio, the M_w does not affect it obviously [57]. As mentioned above, the stretching parameters and the nanofiller addition both have significant influences on the phase transformation and piezoelectricity. Furthermore, they also have co-effects between them. For example, in the stretching of composites, the addition of nanofillers may result in crystal defects (sometimes even visible) more easily than pure PVDF films, so the elongation ratio should be lower. While the phase transformation mechanism in the stretching still remains not so clear, it calls for more efforts from the related researchers.

2.3 Nontraditional stretching

In recent years, besides traditional mechanical stretching, several novel methods have been developed to improve the stretching effects [58,59]. Zhang *et al.* proposed a process combination of simultaneous biaxial stretching and solid-state shear milling (S^3M). Compared to traditional uniaxial stretching, both the relative fraction of the β-phase and the total content of β-phase increase as shown in Figure 7 [24].

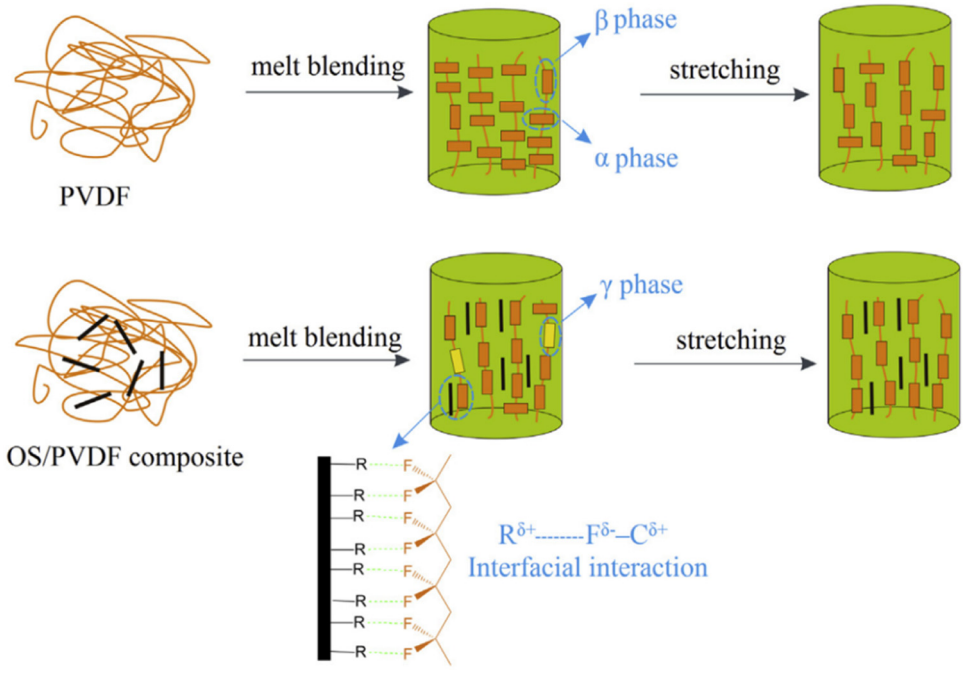

Figure 6: Schematic illustration of the proposed interfacial interaction between PVDF and OS for the improvement of β-phase content in PVDF [20].

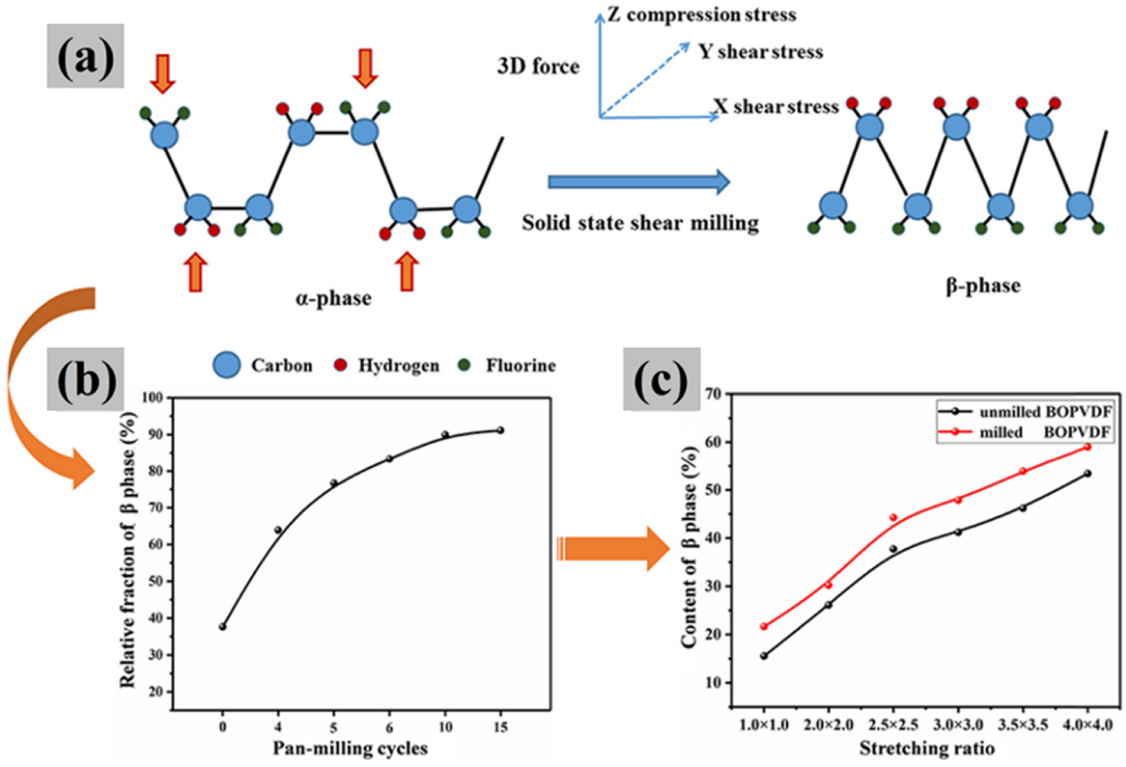

Figure 7: (a) Scheme of conformation conversion of the α-phase to the β-phase in PVDF. (b) The relationship between $F(\beta)$ in PVDF powders and pan-milling cycles. (c) The content of β-phase in milled and unmilled BOPVDF films [24].

Compared to uniaxial stretched films, the biaxial stretched films exhibit more balanced properties. Lu *et al.* applied simultaneous biaxial stretching on PVDF films and investigated its effects on the crystal structure, dielectric properties, and mechanical properties. It attributes to the applied stress during stretching, which forces the alignment of the PVDF molecular chains into the crystals and transforms to the β-phase conformation. As a result, both $F(\beta)$ and X_c increase (unstretched samples: $F(\beta)$ = 39%, X_c = 43%; stretched samples (R = 3.5 × 3.5): $F(\beta)$ = 46%, X_c = 55%). Compared to uniaxially stretched samples, $F(\beta)$ is much higher, which may be caused by the higher stretching temperature and stretching rate [60]. Some researchers suggest that the effect of biaxial stretching is reflected in two aspects: (1) the parallel orientation of PVDF crystals reduces the dielectric loss from the α_c relaxation in α crystal and (2) the biaxial stretching constrains the amorphous phase in PVDF-HFP and thus the migration loss from impurity ions is reduced [61]. Yang *et al.* explored the semi-crystalline structure–dielectric property relationship and the electrical conduction in a biaxially oriented PVDF film under high electric fields and high temperatures. In the work, the film is stretched first along the axial (or extrusion) direction, followed by subsequent stretching using tenter clips along the transverse direction. They found that biaxially oriented PVDF films exhibited a DC breakdown strength as high as biaxially oriented polypropylene films [62]. Kang *et al.* developed a CO_2 laser-heated drawing process to prepare PVDF fibers, as shown in Figure 8. In the experiments, the effects of drawing stress and elongation ratio ((a) 110 MPa, R = 4.5; (b) 220 MPa, R = 5.5) were compared. The structure evolution was observed by *in situ* measurement using synchrotron X-ray radiation. Under a low drawing stress, a moderate neck-deformation occurs, resulting in the mixture of α- and β-phases, in which the β-phase forms within 1 ms after necking,

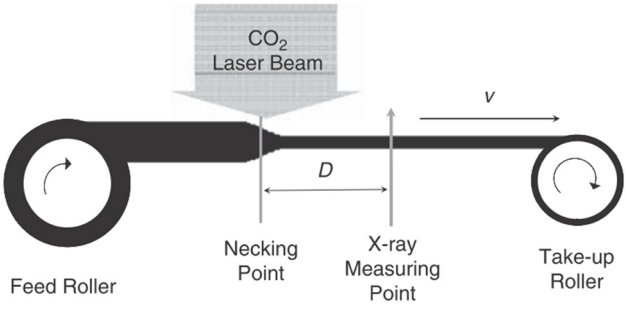

Figure 8: Schematic diagram of the apparatus for CO_2 laser heated-drawing process [63].

earlier than the α-phase. In contrast, under high drawing stress, a steep neck-deformation occurs, resulting in only the β-phase. Small-angle X-ray scattering images showed that meridional streaks appear at low drawing stress, while a four-pointed pattern appears at high drawing stress [63].

Nakamura *et al.* produced α-PVDF films by extrusion with R up to 9 at 160°C (10°C lower than the melting temperature T_m) to obtain β-PVDF films. It was found that nearly all α-phase transformed into the oriented β-phase with increasing R, even when the drawing occurs near T_m. The results indicate that the oriented structure and high F (β) can be attributed to the arrangement of the crystal/amorphous series along the drawing direction [64]. Chen *et al.* prepared high-performance piezoelectric polymer films by simple melt stretching of slightly crosslinked PVDF solution for sensor applications. Upon controlled temperature and stretching ratio, strong chain orientation or extension proceeds prior to crystallization, leading to the generation of an ultrahigh content of polar β-phase (~96%) directly from the melt. The β-phase adopts an oriented nanofibril morphology (with a diameter of 21.6 nm), while the nanofibrils are further densely and parallelly aligned to fill the film space. Attributed to such a nanoscale phase morphology, the melt-stretched PVDF film shows high optical transmittance (~90%), good flexibility, and superior mechanical properties. A flexible piezoelectric device constructed on the β-phase nanofibrils-filled PVDF film is demonstrated to have excellent electrical output in sensing dynamic pressure (0–250 kPa) and temperature variation (3.3 mV/°C) with a broad response range. Figure 9 shows a schematic illustration on the fabrication of PVDF films by a strategy of melt stretching at high temperature, which adopts a three-step process [65].

2.3.1 Simultaneous stretching and poling

In most reports, the stretching and poling processes are independent of each other. In the stretching process, phase transformation finishes completely, and therefore, the effects of poling on phase transformation are not so obvious [35,66]. If stretching and poling are applied simultaneously, better piezoelectricity may be generated. Mahadeva *et al.* applied sequential stretching and corona poling to fabricate piezoelectric PVDF thin films and investigated the effects of poling time and grid voltage on phase transformation and piezoelectricity. It was found that the poling time and grid voltage have no substantial influences on phase transformation, indicating that phase transformation mainly occurs during the stretching process. However, poling has decisive effects on piezoelectricity due to its function on dipole moment alignment [67]. Kumar and Perlman used the simultaneous stretching and corona poling method to fabricate PVDF-TrFE (PVDF/TrFE = 75:25 or 50:50 mol%) copolymer films. The

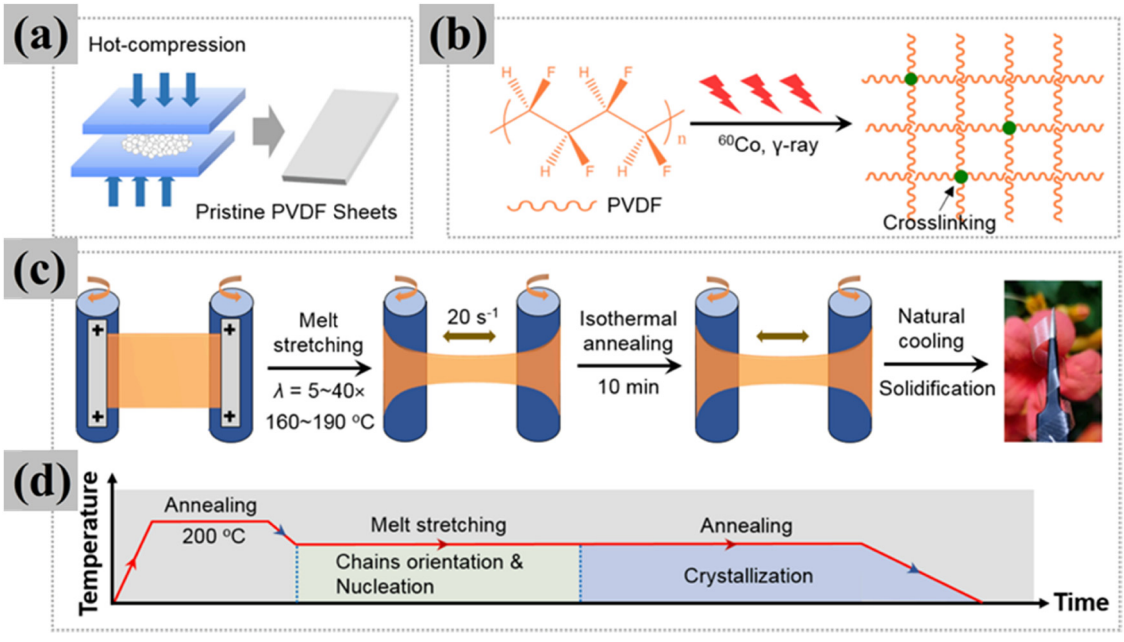

Figure 9: Fabrication of PVDF films by melt stretching. (a) Schematic illustration of vacuum-assisted hot compression to prepare pristine PVDF sheets. (b) Preparation of slightly crosslinked PVDF by γ-ray irradiation. (c) Schematic drawing of home-made two-drum extensional rheometer and the corresponding melt stretching process. The digital photograph of the prepared PVDF film (160°C, 40×) is also shown. (d) Thermal program [64].

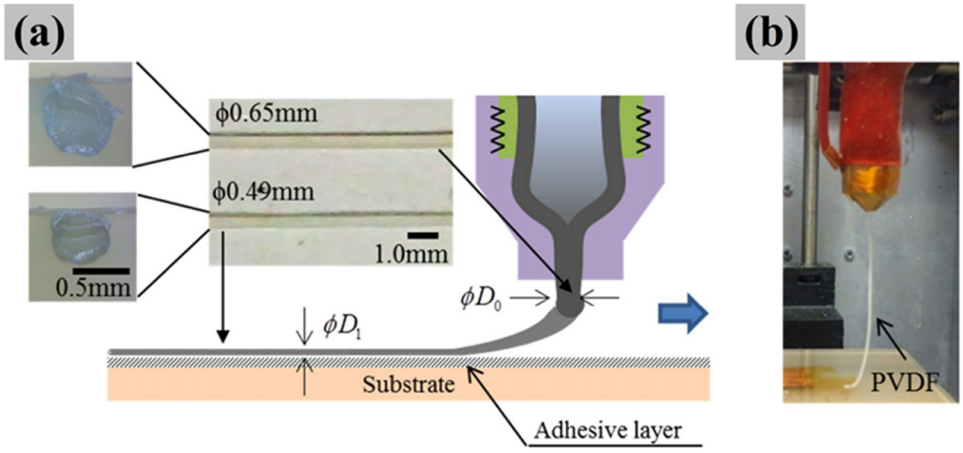

Figure 10: The principle in the proposed printing process of piezoelectric PVDF devices: (a) experimental results of electric poling and the mechanical stretching process in the EPAM process and (b) extrusion results of the filament type of the PVDF polymer [69].

maximum piezoelectric constant d_{31} of 75:25 films reaches 48 pC/N under optimal conditions (R = 4.5, T = 60°C), which is about 1.7 times of those fabricated by separated poling after stretching. The enhancement is attributed to the ferroelectric domain rotation and step rotation of molecular dipoles at 60°C in the field direction. In addition, the optimal poling temperature for PVDF (80°C) is higher than that for PVDF-TrFE (60°C) [68]. Both simultaneous stretching and poling have been utilized in 3D printing techniques in recent years. Lee and Tarbutton utilized an innovative method electric poling-assisted additive manufacturing (EPAM) to print PVDF filament rods under a strong electric field in which poling and stretching are applied simultaneously. Figure 10 shows a schematic of the preparation process. A high electric field is applied to the molten polymer column between the nozzle tip and the printing bed (poling) during extrusion (stretching), which leads to molecular chain alignment and phase transformation to the β-phase [69]. Huan *et al.* developed a simultaneously stretched and static electric poled (SSSEP) process to enhance the piezoelectricity of PVDF-HFP films. The applied apparatus is shown in Figure 11. In this work, the elongation ratio is kept at 4.5, equal to the tooth ratio of Gear 1 and Gear 2, and by varying the poling temperature and the poling electric field, different samples were prepared. The maximum piezoelectric coefficient d_{33} reaches 24 pC/N under optimal conditions (T_p = 65°C, E_{max} = 160 MV/m). From the results, it can also be found that the saturation of the poling electric field is about 150 MV/m [70]. Because of its complexity, the application of the simultaneous stretching and poling method is limited.

2.3.2 Electrospinning

Stretching occurs during the electrospinning process, and therefore, usually no individual stretching is required in

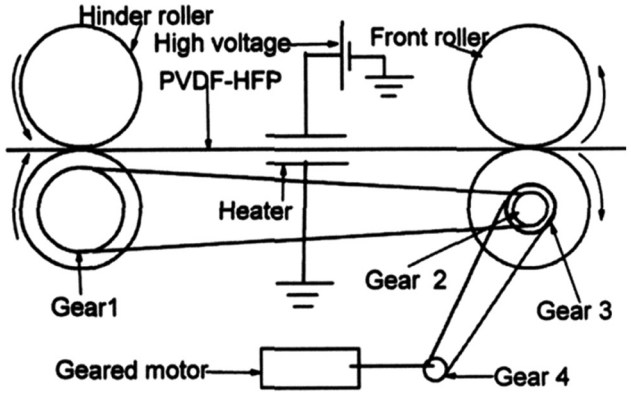

Figure 11: Apparatus of SSSEP for preparing piezoelectric PVDF-HFP films [70].

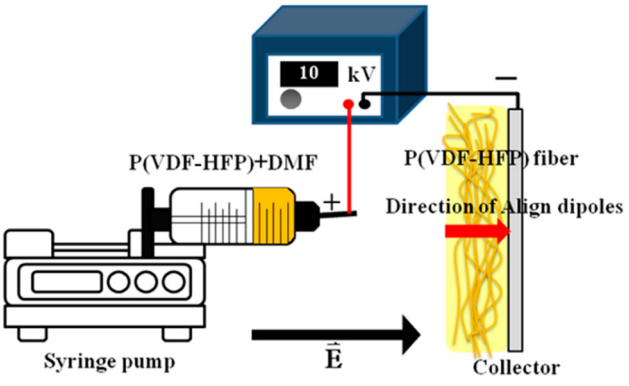

Figure 12: Schematic of the synthesis of PVDF-HFP fibers by the electrospinning process [71].

the preparation of electrospun samples. Figure 12 shows a typical electrospinning process for the preparation of PVDF-HFP fibers [71]. The stress induced by the injection on the mixture solution has a decisive effect on the alignment of the molecular chains as well as the added nanofillers as demonstrated by the electrospinning-hot press method for the preparation of surface modified graphene (SMG)/PVDF composites in Figure 13 [72]. The key parameters of electrospinning are the solvent fraction, tip-to-collector distance (TCD), flow rate, and voltage setting [73]. Gee *et al.* applied the electrospinning method to fabricate piezoelectric nanofiber membranes. By varying the parameters, the optimization setting for piezoelectricity was determined (solvent ratio: 60 vol% DMF + 40 vol% acetone; TCD = 16 cm; flow rate = 0.8 mL/h; voltage setting = 14 kV), at which the β-phase fraction reaches 91.0%. Based on the statistical analysis of the mean β-phase fraction and signal-to-noise ratio, it is concluded that the solvent ratio and flow rate are the two factors contributing most to the β-phase fraction [73]. Similar to traditional stretching, the stretching effect during electrospinning is also affected by the addition of nanofillers. Khalifa *et al.* investigated the synergistic effect of electrospinning and nano-alumina trihydrate (n-ATH) on the crystal structure and piezoelectric properties of PVDF nanofibers. The added n-ATH can enhance the surface of the electrospun droplets, which leads to the decrease in the thickness. When the n-ATH increases to 10%, $F(\beta)$ reaches the highest value of 70.1% and the highest output voltage of 840 mV, both of which are much higher than those of pure PVDF nanofibers. When the n-ATH content is above 10%, $F(\beta)$ decreases, which may be attributed to the dilution effect [74]. Lei *et al.* investigated the dipole arrangement during electrospinning. Compared with mechanical spinning, the electrospun fibers can generate voltage after deformation, while the mechanical-spun fibers do not exhibit piezoelectricity. This result indicates that although both processes can produce high-β-fraction PVDF fibers, the applied voltage during electrospinning can force the dipole moments along the electric field, and thus exhibit piezoelectricity. For mechanical-spun fibers, the dipole moments are randomly distributed, and thus the fibers have no piezoelectricity. In other words, electrospinning includes both stretching and poling functions [75]. Lei *et al.* developed an electrospinning process to produce PVDF membranes of desired phases by simultaneously controlling the collector temperature and the flow rate during electrospinning. The α-, β- or γ-phase dominant PVDF nanofibrous membranes can be achieved by adjusting the electrospinning parameters and heat treatment during or after electrospinning [76]. The influences of the parameters can be described briefly as follows: (a) the voltage can influence the nanofiber creation and the formation of the β-phase to some extent, and an excessively high voltage may lead to instability of jets and decrease the solvent evaporation rate; (b) TCD influences the diameter of the nanofibers (the lager the TCD, the smaller the diameter); (c) high feed rate can lead to the formation of the β-phase and uniform fibers, while excessively high rates create unstable jets and

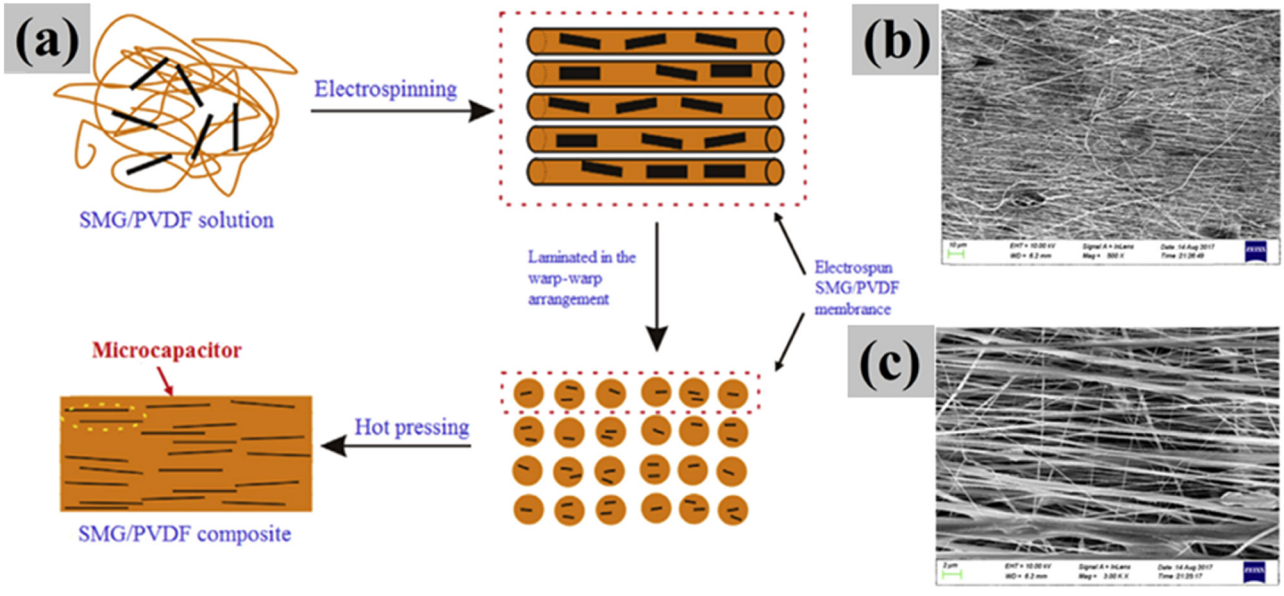

Figure 13: (a) The preparation process of SMG/PVDF composites by an electrospinning-hot pressing method. SEM images of electrospun SMG (16 wt%)/PVDF membrane at (b) low and (c) high magnification [72].

Table 1: A brief summary of stretching effects on the β-phase formation of PVDF and its copolymers

Factors	Positive effect	Negative effect	Remarks
Temperature	Eliminate the internal stress and improve the ductility [32]	When the temperature is above 100°C, the phase transformation decreases or even disappears At higher temperatures, the weaker filler–matrix compatibility and higher chain mobility limit the phase transformation [35]	The appropriate T_s is usually set from 60 to 100°C
Elongation rate	Increase the crystallinity (possible) [42,46]	Decrease the crystallinity (possible) [23]	The elongation is set from 3 to 5
Speed	Improve the transformation from α- to β-phase (high speed) [47]	Lower phase transformation efficiency [48,49] Decreases the crystallinity degree (high speed) [50,51]	
Nanofiller addition	Improve phase transformation due to the stress concentration on the PVDF/nanofiller interface [20,22] Increase the dielectric constant [22] Increase the crystallinity degree [20]	Reduces the crystallinity induced by phase transformation and nanofiller re-orientation [22,23] Extremely lower content nanofillers (<threshold value) may hinder phase transformation [22] The agglomeration of nanofillers at higher concentrations results in chain confinement, thus leading to lower piezoelectricity [23]	
Simultaneous stretching and poling	Molecular chain alignment and β-phase formation [69] Molecular dipole moments rotation [68]	Complicate operation	T_p > 60°C, R > 4, E_{max} > 150 MV/m

disruption of electrospinning; and (d) solvent fraction can influence the solution viscosity and the nanofiber diameter, while it may lead to electrospraying and exhibit negative effects on the β-phase formation if the solvent fraction is too high [77–83]. Yang *et al.* added GO into PVDF to prepare nanofiber mats by electrospinning. By heating the PVDF/GO nanofiber mat at 140°C for 1 h, the PVDF/rGO mat was produced by the reduction of GO to rGO. The β-phase content was improved with the GO (or rGO) content until 2 wt%, and therefore, the power generation capability was increased. Compared to PVDF/GO, the output voltage of PVDF/rGO was higher due to fewer functional groups on the carbon atoms [84]. In addition, it was reported that natural substances were added into PVDF. Lee *et al.* prepared PVDF/cellulose nanocrystal (CNC) nanocomposite fibers (CNC content: 0, 1, and 3 wt%) by dry-jet wet spinning, followed by mechanical stretching with the drawing ratio R = 8. The fraction of β-phase appears to be slightly higher in CNC containing as-spun nanocomposite fibers, which may be due to the synergistic effect of a low stretching degree and heterogeneous nucleation. When R = 8, all polymer chains are supposed to be highly aligned and thereby the fraction of β-phase dramatically increases. However, the PVDF/CNC (3 wt%) composites had a 10% lower β-fraction and instead contained more γ phase because of the hindrance caused by the defects during the β-phase formation [85]. Issa *et al.* studied the physicomechanical properties of electrospun PVDF/cellulose nanofibers. It was found that the hydroxyl groups on cellulose would force the molecular chains in PVDF to be in the trans-conformation, during which the cellulose particles could act as nucleation agents. Moreover, the total crystallinity degree and the formation of β-crystals were improved mainly by the molecular chains and crystal orientation in electrospinning, while a little additional contribution from the cellulose dispersed in the electrospun PVDF [86].

From these studies, it is evident that electrospinning is a suitable method to produce piezoelectric fibers or films of low thickness.

3 Summary

The influences of stretching on phase transformation are investigated and the results are summarized in Table 1. It is worth noting that the parameters of stretching are not independent of each other on the properties of the materials. As a result, during the development of a suitable method for PVDF or its copolymers, a lot of work has to be done before the optimization parameters can be determined. Another point noteworthy noting is that the effect of one parameter reported in one study may differ from that of other reports, or even be contradictory.

4 Conclusions

Stretching is an important method to improve the α- to β-phase transformation efficiently in PVDF films. In this work, the effects of stretching parameters (temperature, elongation ratio, stretching speed, and nanofiller addition) are discussed. It is worth noting that for most parameters, there is a proper value at which the optimal effects can be achieved. Another aspect that should be pointed out is that the effects are clearly influenced by specific conditions. For example, in some reports, the crystallinity degree increases after stretching, while in others, completely different results are observed. In addition, the nontraditional stretching method is introduced briefly. This work can help researchers in the piezoelectric polymer field to understand the mechanism of phase transformation during stretching and to fabricate high piezoelectric polymer/composite films.

Funding information: This work was financially supported by the National Natural Science Foundation of China (No. 51703015) and Fundamental Research Funds for the Central Universities (No. 2020CDJQY-A008).

Author contributions: All authors have accepted responsibility for the entire content of this manuscript and approved its submission.

Conflict of interest: The authors state no conflict of interest.

Data availability statement: The datasets generated and/or analysed during the current study are available from the corresponding author on reasonable request.

References

[1] Cui ZL, Hassankiadeh NT, Zhuang YB, Drioli E, Lee YM. Crystalline polymorphism in poly(vinylidenefluoride) membranes. Prog Polym Sci. 2015;51:94–126.

[2] Katsouras I, Asadi K, Li MY, van Driel TB, Kjaer KS, Zhao D, et al. The negative piezoelectric effect of the ferroelectric polymer poly (vinylidene fluoride). Nat Mater. 2016;15(1):78–84.

[3] Correia HMG, Ramos MMD. Quantum modelling of poly(vinylidene fluoride). Comput Mater Sci. 2005;33(1–3):224–9.

[4] Martins P, Lopes AC, Lanceros-Mendez S. Electroactive phases of poly(vinylidene fluoride): Determination, processing and applications. Prog Polym Sci. 2014;39(4):683–706.

[5] Ribeiro C, Costa CM, Correia DM, Nunes-Pereira J, Oliveira J, Martins P, et al. Electroactive poly(vinylidene fluoride)-based structures for advanced applications. Nat Protoc. 2018;13(4):681–704.

[6] Chamakh MM, Mrlík M, Leadenham S, Bažant P, Osička J, AlMaadeed MAA, et al. Vibration sensing systems based on poly (vinylidene fluoride) and microwave-assisted synthesized ZnO star-like particles with controllable structural and physical properties. Nanomaterials. 2020;10(12):1–15.

[7] Wan CY, Bowen CR. Multiscale-structuring of polyvinylidene fluoride for energy harvesting: The impact of molecular-, micro- and macro-structure. J Mater Chem A. 2017;5:3091–128.

[8] Wu Y, Hsu SL, Honeker C, Bravet DJ, Williams DS. The role of surface charge of nucleation agents on the crystallization behavior of poly (vinylidene fluoride). J Phys Chem B. 2012;116(24):7379–88.

[9] Dadi S, Paul R, Michael W. The step-wise poling of VDF/TrFE copolymers. Ferroelectrics. 1996;186:255–8.

[10] Sencadas V, Gregorio R, Lanceros-Méndez S. α to β-phase transformation and microestructural changes of PVDF films induced by uniaxial stretch. J Macromol Sci-Phys. 2009;48(3):514–25.

[11] Ting Y, Gunawan H, Sugono A, Chiu CW. A new approach of polyvinylidene fluoride (PVDF) poling method for higher electric response. Ferroelectrics. 2013;446(1):28–38.

[12] Lam TN, Wang CC, Ko WC, Wu JM, Lai SN, Chuang WT, et al. Tuning mechanical properties of electrospun piezoelectric nanofibers by heat treatment. Materialia. 2019;8:100461.

[13] Ren JY, Ouyang QF, Ma GQ, Li Y, Lei J, Huang HD, et al. Enhanced dielectric and ferroelectric properties of poly(vinylidene fluoride) through annealing oriented crystallites under high pressure. Macromolecules. 2022;55(6):2014–27.

[14] Kim GH, Hong SM, Seo Y. Piezoelectric properties of poly(vinylidene fluoride) and carbon nanotube blends: β-phase development. Phys Chem Chem Phys. 2009;11(44):10506–12.

[15] Furukawa T. Ferroelectric properties of vinylidene fluoride copolymers. Phase Transit. 1989;18:143–211.

[16] Florczak S, Lorson T, Zheng T, Mrlik M, Hutmacher DW, Higgins MJ, et al. Melt electrowriting of electroactive poly (vinylidene difluoride) fibers. Polym Int. 2019;68(4):735–45.

[17] Kade JC, Bakirci E, Tandon B, Gorgol D, Mrlik M, Luxenhofer R, et al. The impact of including carbonyl iron particles on the melt electrowriting process. Macromol Mater Eng. 2022;307(12):2200478.

[18] Li L, Zhang MQ, Rong MZ, Ruan WH. Studies on the transformation process of PVDF from α to β phase by stretching. RSC Adv. 2014;4(8):3938–43.

[19] Tang CW, Li B, Sun LL, Lively B, Zhong WH. The effects of nanofillers, stretching and recrystallization on microstructure, phase transformation and dielectric properties in PVDF nanocomposites. Eur Polym J. 2020;48(6):1062–72.

[20] He FA, Lin K, Shi DL, Wu HJ, Huang HK, Chen JJ, et al. Preparation of organosilicate/PVDF composites with enhanced piezoelectricity and pyroelectricity by stretching. Compos Sci Technol. 2016;137:138–47.

[21] Lee S. Carbon nanofiber/poly(vinylidene fluoride-hexafluoro propylene) composite films: The crystal structure and thermal properties with various stretching temperatures. Fibers Polym. 2013;14(3):441–6.

[22] Sun LL, Li B, Zhang ZG, Zhong WH. Achieving very high fraction of β-crystal PVDF and PVDF/CNF composites and their effect on AC conductivity and microstructure through a stretching process. Eur Polym J. 2010;46(11):2112–9.

[23] Mishra S, Sahoo R, Unnikrishnan L, Ramadoss A, Mohanty S, Nayak SK. Investigation of the electroactive phase content and dielectric behaviour of mechanically stretched PVDF-GO and PVDF-rGO composites. Mater Res Bull. 2020;124:110732.

[24] Zhang HL, Lu HC, Liu ZG, Li L. Preparation of high-performance polyvinylidene fluoride films by the combination of simultaneous

biaxial stretching and solid-state shear milling technologies. Ind Eng Chem Res. 2020;59(41):18539–48.
[25] da Silva AB, Wisniewski C, Esteves JVA, Gregorio R. Effect of drawing on the dielectric properties and polarization of pressed solution cast β-PVDF films. J Mater Sci. 2010;45(15):4206–15.
[26] Progreb R, Whyman G, Musin A, Stanevsky O, Bormashenko Y, Sternklar S, et al. The effect of controlled stretch on luminescene of $Eu(III)(NO_3)_3$(*o*-Phen)$_2$ complex doped into PVDF film. Mater Lett. 2006;60(15):1911–4.
[27] Mun J, Park HM, Koh E, Lee YT. Enhancement of the crystallinity and surface hydrophilicity of a PVDF hollow fiber membrane on simultaneous stretching and coating method. J Ind Eng Chem. 2018;65:112–9.
[28] McGrath JC, Ward IM. High effective draw as route to increased stiffness and electrical response in poly(vinyliudene fluoride). Polymer. 1980;21(8):855–7.
[29] Hsu TC, Geil PH. Deformation and transformation mechanisms of poly(vinylidene fluoride) (PVF_2). J Mater Sci. 1989;24(4):1219–62.
[30] Chinaglia DL, Gregorio R, Vollet DR. Structural modification in stretch-induced crystallization in PVDF films as measured by small-angle X-ray scattering. J Appl Polym Sci. 2011;125(1):527–35.
[31] Kim TH, Jee KY, Lee YT. The improvement of water flux and mechanical strength of PVDF hollow fiber membranes by stretching and annealing conditions. Macromol Res. 2015;23(7):592–600.
[32] Sencadas V, Gregorio R, Lanceros-Mendez S. α to β phase transformation and microstructural changes of PVDF films induced by uniaxial stretch. J Macromol Sci Part B – Phys. 2009;48(3):514–25.
[33] Ting Y, Suprapto, Chiu C, Gunawan H. Characteristics analysis of biaxially stretched PVDF thin films. J Appl Polym Sci. 2018;135(36):46677.
[34] Debili S, Gasmi A, Bououdina M. Synergistic effects of stretching/polarization temperature and electric field on phase transformation and piezoelectric properties of polyvinylidene fluoride nanofilms. Appl Phys A – Mater Sci Process. 2020;126(4):309.
[35] Guo HL, Li JQ, Meng YF, Christiansen JD, Yu DH, Wu ZH, et al. Stretched-induced stable-metastable crystal transformation of PVDF/graphene composites. Polym Cryst. 2019;2(4):e10079.
[36] Wang JT, Chen Z, Wang YQ, Chu YF, Pan M, Dong LJ. Effect of uniaxial tension on piezoelectric response of PVDF Film. Acta Poly Sin. 2020;51(12):1367–73.
[37] Zhang XL, Xiao CF, Hu XY, Bai QQ. Preparation and properties of homogeneous-reinforced polyvinylidene fluoride hollow fiber membrane. Appl Surf Sci. 2013;264:801–10.
[38] Zhou Y, Liu WT, Tan B, Zhu C, Ni YR, Fang L, et al. Crystallinity and β phase fraction of PVDF in biaxially stretched PVDF/PMMA films. Polymer. 2021;13(7):998.
[39] Chang WY, Fang TH, Liu SY, Lin YC. Phase transformation and thermomechanical characteristics of stretched polyvinylidene fluoride. Mater Sci Eng A. 2008;480(1–2):477–82.
[40] Ji DW, Xiao CF, An SL, Chen KK, Gao YF, Zhou F, et al. Completely green and sustainable preparation of PVDF hollow fiber membranes via melt-spinning and stretching method. J Hazard Mater. 2020;398:122823.
[41] Ozkazanc E, Guney HY. The variation of the dielectric constant and loss index with temperature and draw ratio in α-PVDF. J Appl Polym Sci. 2009;112(4):2482–5.
[42] Ozkazanc E, Guney HY, Oskay T, Tarcan E. The effect of uniaxial orientation on the dielectric relaxation behavior of α-PVDF. J Appl Polym Sci. 2008;109(6):3878–86.
[43] Jahan N, Mighri F, Rodrigue D, Aiji A. Enhanced electroactive β phase in three phase PVDF/$CaCO_3$/nanoclay composites: Effect of micro-$CaCO_3$ and uniaxial stretching. J Appl Polym Sci. 2017;134(24):44940.
[44] Wang H, Chen QS, Xia W, Qiu XL, Cheng Q, Zhu GD. Electroactive PVDF thin films fabricated via cooperative stretching process. J Appl Polym Sci. 2018;135(22):46324.
[45] Jain A, Kumar JS, Srikanth S, Rathod VT, Mahapatra DR. Sensitivity of polyvinylidene fluoride films to mechanical vibration modes and impact after optimizing stretching conditions. Polym Eng Sci. 2013;53(4):707–15.
[46] Magniez K, Krajewski A, Neuenhofer M, Helmer R. Effect of drawing on the molecular orientation and polymorphism of melt-spun polyvinylidene fluoride fibers: Toward the development of piezoelectric force sensors. J Appl Polym Sci. 2013;129(5):2699–705.
[47] Lei CH, Hu B, Xu RJ, Cai Q, Shi WQ. Influence of room-temperature-stretching technology on the crystalline morphology and microstructure of PVDF hard elastic film. J Appl Polym Sci. 2014;131(7):2699–705.
[48] Perlman MM. Method to double the piezo- and pyroelecric of polyvinylidene fluoride (PVDF) films. US Patent. US5254296; 1993.
[49] Sobhani H, Razavi-Nouri M, Yousefi AK. Effect of flow history on poly(vinylidene fluoride) crystalline phase transformation. J Appl Polym Sci. 2007;104(1):89–94.
[50] Lee SH, Cho HH. Crystal structure and thermal properties of poly (vinylidene fluoride)-carbon fiber composite films with various stretching temperature and speeds. Fibers Polym. 2010;11(8):1146–51.
[51] Tang YH, Lin YK, Lin HH, Li CY, Zhou B, Wang XL. Effects of room temperature stretching and annealing on the crystallization behavior and performance of polyvinylidene fluoride hollow fiber membranes. Membranes. 2020;10(3):38.
[52] Mishra S, Sahoo R, Unnikrishnan L, Ramadoss A, Mohanty S, Nayak SK. Enhanced structural and dielectric behaviour of PVDF-PLA binary polymeric blend system. Mater Today Commun. 2021;26:101958.
[53] Sodagar S, Jaleh B, Fakhri P, Kashfi M, Mohazzab B, Feizi Momeni A. Flexible piezoelectric PVDF/NDs nanocomposite films: improved electroactive properties at low concentration of nanofiller and numerical simulation using finite element method. J Polym Res. 2020;59(41):18539–48.
[54] Sun LL, Wu N, Peng R. Effect of stretching process on crystalline structures and alternating current conductivity of CNF/PVDF composites. Cailiao Gongcheng-J Mater Eng. 2020;48(6):106–11.
[55] Yan JJ, Xiao CF, Huang Y, Zhang T. Study of crystal structure and properties of poly(vinylidene fluoride)/graphene composite fibers. Polym Int. 2021;71(1):26–37.
[56] Yu LJ, Li WP. Stretching-induced percolation in polyvinylidene fluoride and nickel composites. J Appl Polym Sci. 2011;120(4):2368–73.
[57] Mrlík M, Osička, Cvek M, Ilčíková M, Srnec P, Gorgol D, et al. Comparative study of PVDF sheets and their sensitivity to mechanical vibrations: The role of dimensions, molecular weight, stretching and poling. Nanomaterials. 2021;11(7):1637.
[58] Yang RL, Li JM, Wang Y, Liu Y, Du XS, Li WZ. Pyroelectric polyvinylidene fluoride film prepared by a novel combining method and its application in fully flexible infrared detector. Infrared Phys Technol. 2021;113:103624.
[59] Tao R, Shi JH, Rafiee M, Akbarzadeh A, Therriault D. Fused filament fabrication of PVDF films for piezoelectric sensing and energy harvesting applications. Mater Adv. 2022;3(12):4851–60.

[60] Lu HC, Li L. Crystalline structure, dielectric, and mechanical properties of simultaneously biaxially stretched polyvinylidene fluoride film. Polym Adv Technol. 2018;29(12):3056–64.
[61] Yin K, Zhou Z, Schuele DE, Wolak M, Zhu L, Baer E. Effects of interphase modification and biaxial orientation on dielectric properties of poly(ethylene terephthalate)/poly(vinylidene fluoride-co-hexafluoropropylene) multilayer films. ACS Appl Mater Interfaces. 2016;8(21):13555–66.
[62] Yang LY, Ho J, Allahyarov E, Mu R, Zhu L. Semicrystalline structure dielectric property relationship and electrical conduction in biaxially oriented poly(vinylidene fluoride) film under high electric fields and high temperatures. ACS Appl Mater Interfaces. 2015;7(36):19894–905.
[63] Kang YA, Kim KH, Ikehata S, Ohkoshi Y, Gotoh Y, Nagura M, et al. Development of a fiber structure in poly(vinylidenne fluoride) by a CO_2 laser-heated drawing process. Polym J. 2010;42(8):657–62.
[64] Nakamura K, Nagai M, Kanamoto T, Takahashi Y, Furukawa T. Development of oriented structure and properties on drawing of poly(vinylidene fluoride) by solid-state coextrusion. J Polym Sci Part B. 2011;39(12):1371–80.
[65] Chen B, Yuan M, Ma RX, Wang XH, Cao W, Liu CT, et al. High performance piezoelectric polymer film with aligned electroactive phase nanofibrils achieved by melt stretching of slightly cross-linked poly (vinylidene fluoride) for sensor applications. Chem Eng J. 2022;433(1):134475.
[66] Yang J, Yao XH, Meng ZX. Investigation of molecular mechanisms of polyvinylidene fluoride under the effects of temperature, electric poling, and mechanical stretching using molecular dynamics simulations. Polymer. 2022;245:124691.
[67] Mahadeva SK, Berring J, Walus K, Stoeber B. Effect of poling time and grid voltage on phase transition and piezoelectricity of poly (vinylidene fluoride) thin films using corona poling. J Phys D – Appl Phys. 2013;46(28):285305.
[68] Kumar A, Perlman MM. Simultaneous stretching and corona poling of PVDF and P(VDF-TriFe) films. II. J Phys D – Appl Phys. 1993;26(3):469–73.
[69] Lee C, Tarbutton JA. Electric poling-assisted additive manufacturing process for PVDF polymer-based piezoelectric device applications. Smart Mater Struct. 2014;23(9):095044.
[70] Huan Y, Liu YY, Yang YF. Simultaneous stretching and static electric field poling of poly(vinylidene fluoride-hexafluoropropylene) copolymer films. Polym Eng Sci. 2007;47(10):1630–3.
[71] Tohluebaji N, Putson C, Muensit N. High electromechanical deformation based on structural beta-phase content and electrostrictive properties of electrospun poly(vinylidene fluoride-hexafluoropropylene) nanofibers. Polymer. 2019;11(11):1187.
[72] Lin B, Li ZT, Yang Y, Li Y, Lin JC, Zheng XM, et al. Enhance dielectric permittivity in surface-modified graphene/PVDF composites prepared by an electrospinning-hot pressing method. Compos Sci Technol. 2019;172:58–65.
[73] Gee S, Johnson B, Smith AL. Optimizing electrospinning parameters for piezoelectric PVDF nanofiber membranes. J Membr Sci. 2018;563:804–12.
[74] Khalifa M, Deeksha B, Mahendran A, Anandhan S. Synergism of electrospinning and nano-alumina trihydrate on the polymorphism, crystallinity and piezoelectric performance of PVDF nanofibers. Jom. 2018;70(7):1313–8.
[75] Lei TP, Yu LK, Zheng GF, Wang LY, Wu DZ, Sun DH. Electrospinning-induced preferred dipole orientation in PVDF fibers. J Mater Sci. 2015;50(12):4342–7.
[76] Lei TP, Zhu P, Cai XM, Yang L, Yang F. Electrospinning of PVDF nanofibrous membranes with controllable crystalline phases. Appl Phys A. 2015;120(1):5–10.
[77] Kalimuldina G, Turdakyn N, Abay I, Medeubayev A, Nurpeissova A, Adair D, et al. A review of piezoelectric PVDF film by electrospinning and its applications. Sensors. 2020;20(18):5214.
[78] Zhao ZZ, Li JQ, Yuan XY, Li X, Zhang YY, Sheng J. Preparation and properties of electrospun poly(vinylidene fluoride) membranes. J Appl Polym Sci. 2005;97(2):466–74.
[79] Zaarour B, Zhang WX, Zhu L, Jin XY. Maneuvering surface structures of polyvinylidene fluoride nanofibers by controlling solvent systems and polymer concentration. Text Res J. 2019;89(12):2406–22.
[80] Costa LMM, Bretas RES, Gregorio R. Effect of solution concentration on the electrospray/electrospinning transition and on the crystalline phase of PVDF. Mater Sci Appl. 2010;1(4):247–52.
[81] Shao H, Fang J, Wang HX, Lin T. Effect of electrospinning parameters and polymer concentration on mechanical-to-electrical energy conversion of randomly-oriented electrospun poly(vinylidene fluoride) nanofibers mats. RSC Adv. 2015;5(19):14345–50.
[82] Matabola KP, Moutloali RM. The influence of electrospinning parameters on the morphology and diameter of poly(vinylidene fluoride) nanofibers-effect of sodium chloride. J Mater Sci. 2013;48(16):5475–82.
[83] Zulfikar MA, Afrianingsih I, Nasir M, Alni A. Effect of processing parameters on the morphology of PVDF electrospun nanofiber. In 2018 IOP Journal of Physics Conference series: Applied Nanotechnology and Nanoscience International Conference. Vol. 987; 2017. p. 012011.
[84] Yang J, Zhang Y, Li Y, Wang Z, Wang W, An Q, et al. Piezoelectric nanogenerators based on graphene oxide/PVDF electrospun nanofiber with enhanced performances by in-situ reduction. Mater Today Commun. 2021;26:101629.
[85] Lee J, Shin Y, Lee G, Kim J, Ko H, Chae HG. Polyvinylidene fluoride (PVDF)/cellulose nanocrystal (CNC) nanocomposite fiber and triboelectric textile sensors. Compos Part B-Eng. 2021;223:109098.
[86] Issa AA, Al-Maadeed MAAS, Mrlík M, Luyt AS. Electrospun PVDF graphene oxide composite fibre mats with tunable physical properties. J Polym Res. 2016;23:1–13.